Effect of the cyclic prefix on the timing synchronization method in ACO-OFDM systems

Shuang Tian, Kusha Panta, Brendon Schmidt and Jean Armstrong
Department of Electrical and Computer Systems Engineering
Monash University, Clayton, VIC 3800, Australia
Tel: +61 3 9905 5355, Fax: +61 3 9905 3454
E-mail: shuang.tian@eng.monash.edu.au

***Abstract*—Recently, a new timing synchronization method for optical wireless systems using asymmetrically clipped optical OFDM (ACO-OFDM) has been proposed. The synchronization method makes use of a novel training symbol and its autocorrelation properties for timing offset estimation via a timing metric. In this paper, we will discuss the effect of the length of cyclic prefix (CP) on the detection of the maximum and minimum of the timing metric. We show that the performance of the timing offset estimation scheme based on maximum detection is affected by the length of the CP while the scheme based on minimum detection of the metric is less sensitive to the CP length. Simulation results are presented to demonstrate the effect of the CP in both detection criteria.**

I. INTRODUCTION

Orthogonal frequency division multiplexing (OFDM) has been used in many radio frequency (RF) based communication applications because of its high spectral efficiency and simple hardware implementation. OFDM has also been considered for optical systems as a candidate for future short range high data rate communication systems [1, 2] as optical wireless systems are low cost and have no spectrum restrictions.

The signals used in optical wireless links are intensity modulated (IM) and hence the transmitted signals must be non-negative. However, normal OFDM (RF-Based) signals are bipolar, and until recently all IM optical-OFDM systems have used a DC bias to move bipolar signals to be all positive [3]. DC biased optical OFDM (DCO-OFDM) requires a high optical power and is not suited to typical applications where the transmitted optical power is limited by eye safety considerations. Recent work [1, 4] has led to the development of a new power efficient form of optical OFDM, called the asymmetrically clipped optical OFDM (ACO-OFDM) that clips particular classes of bipolar OFDM signals. ACO-OFDM retains all of the other attractive properties of OFDM systems.

Due to the sensitivity of OFDM based systems to synchronization errors, ACO-OFDM needs effective synchronization techniques. This paper focuses on the issue of timing synchronization based on specially designed training symbols. The objective of timing synchronization methods is to find the start of transmitted OFDM symbols so that they can be demodulated with FFT at the receiver without any intersymbol interference (ISI). A large number of timing synchronization methods have been proposed in the literature for RF-based OFDM systems, see [5-7] and references therein. However, these methods cannot be applied directly to ACO-OFDM systems where signals have to satisfy a number of properties. These properties will be included in Section II. Recently, a synchronization method based on a novel training symbol has been proposed for ACO-OFDM [8]. In this paper, we will discuss the effect of the cyclic prefix (CP) length on the performance of this method. It will be shown that the performance of the synchronization method based on the detection of the maximum of the timing metric is affected by the choice of the CP length whereas that of minimum is not. Simulation results are included to show the performance of maximum and minimum detection schemes in ACO-OFDM systems.

The rest of the paper is organized as follows. In Section II an ACO-OFDM system is introduced. Section III describes the new synchronization method proposed in [8] for ACO-OFDM systems. Section IV discusses the effect of CP length on two different detection schemes that can be used for timing offset estimation. Simulation results comparing the performance of different estimators in terms of the mean and variance are included in Section V. Finally some concluding remarks are made in Section VI.

II. AN ACO-OFDM SYSTEM

Fig. 1 shows the block diagram of an optical wireless communication system using ACO-OFDM. The data to be transmitted is first mapped onto complex numbers from the constellation being used, e.g. 4-QAM or 16-QAM. These complex numbers are then mapped onto $\mathbf{S}$, where $\mathbf{S} = S(0)\cdots S(N-1)$ is the vector of length N which is input to the inverse fast Fourier transform (IFFT). $\mathbf{S}$ has Hermitian symmetry so that data, $\mathbf{s} = s(0)\cdots s(N-1)$, at the output of the IFFT is real. At the IFFT output, the CP is then inserted and the data is parallel-to-serial converted. The resulting

signal is clipped at zero to give unipolar samples $x(n)$ which are converted to analog, filtered and used to intensity modulate the optical source. The optical signal that is transmitted is $x(t)$. In the form of ACO-OFDM which is considered here, only odd frequency subcarriers are used to carry data, i.e. $S(k)=0$ for k even. The Hermitian constraint and the use of only odd subcarriers to carry data mean that there are only $N/4$ independent complex inputs to the IFFT in each ACO-OFDM symbol. This would be extremely inefficient in an RF-OFDM system. However, ACO-OFDM has been shown to be a very efficient optical modulation technique given the unipolar constraint on the transmitted signal and the fact that optical power depends on $E[x(n)]$ rather than $E[x^2(n)]$ in intensity modulated systems [10]. The ACO-OFDM signal is then transmitted via an optical channel and received by a photodetector. The rest of the receiver structure for ACO-OFDM is similar to that of a conventional RF-OFDM system [4, 5].

The received serial baseband samples $r(n)$ are given by [9]

$$r(n) = x(n) \otimes h(n) + w(n) \tag{1}$$

where " $\otimes$ " denotes convolution, $h(n)$ is the sampled impulse response of the optical channel, $w(n)$ is additive white Gaussian noise (AWGN).

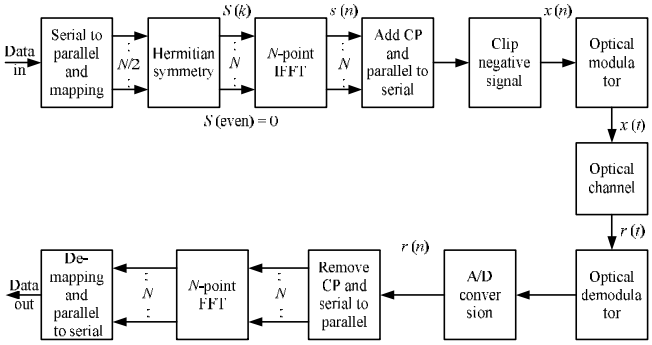

Fig. 1 Block diagram of an ACO-OFDM system.

III. TIMING SYNCHRONIZATION IN ACO-OFDM

Most existing timing synchronization techniques are based on the autocorrelation properties of special training symbols which are embedded in the OFDM signals; and the aim of the timing synchronization methods is to find the start position of the training symbol [5-7], as shown in Fig. 2,

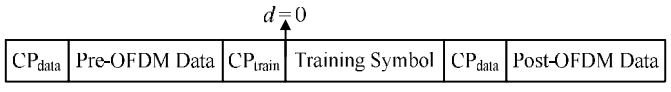

Fig. 2 Time domain OFDM symbol.

where d is a time index and $d=0$ represents the start point of the training symbol. The start of the training symbol is then used to find the start of OFDM symbol frames so that FFT window can be applied across them.

The existing methods give satisfactory timing performance in RF-OFDM. However, they cannot be used directly in ACO-OFDM, because the training symbols they require are bipolar and complex; in addition, some of these methods use only the even subcarriers and some use both even and odd subcarriers to build training symbols. Such training symbols do not satisfy the constraints of the ACO-OFDM symbols. Therefore, a training symbol and timing metric which are tailored to ACO-OFDM have been proposed in [8] and are summarized below. Moreover, in this section, two detection schemes, Maximum and Minimum Detection are considered for the purpose of timing offset estimation; and the effect of the length of the CP on the performance of these schemes is discussed.

A. *Training Symbol*

The training symbol (before clipping) has the form

$$\mathrm{s} = \left[s_0 \quad C_{N/4-1} \quad 0 \quad -C_{N/4-1}^{mirror} \quad -s_0 \quad -C_{N/4-1} \quad 0 \quad C_{N/4-1}^{mirror} \right] \tag{2}$$

where $C_{N/4-1}$ is a real-valued sequence of length $N/4-1$ and $C_{N/4-1}^{mirror}$ is the mirror image of $C_{N/4-1}$. This training symbol has three important properties: it is real, it has Hermitian symmetry and $s(n+N/2) = -s(n)$. To generate a time domain symbol with each of these three properties using an IFFT, the frequency domain vector S at the IFFT input must have Hermitian symmetry; it must be real and $S(k)=0$ for k even. In this paper we consider the case where S is a real binary sequence; in other words the training symbol uses BPSK modulation. There is no constraint on the constellations for data symbols for example 4-QAM or 16-QAM could be used.

The training symbol is the IFFT output of a BPSK PN sequence. To simplify the analysis, we assume $s_0 = 0$. The training symbol after clipping is given by

$$\mathbf{x}_{train} = \left[0 \quad C_{clip} \quad 0 \quad \left(-C^{mirror}\right)_{clip} \quad 0 \quad \left(-C\right)_{clip} \quad 0 \quad \left(C^{mirror}\right)_{clip} \right] \tag{3}$$

where, for simplicity the subscript $N/4-1$ has been omitted and where C_{clip} is the sequence which is the result of clipping $C_{N/4-1}$ to zero. Note that $-C_{clip} \neq \left(-C\right)_{clip}$. It should also be noted that the training symbol is a special format of an ACO-OFDM data symbol and hence can also be used for channel estimation and be generated using the same hardware as the ACO-OFDM data symbols.

B. Timing Metric

Given the training symbol of (3), the timing metric used to detect the start of the training symbol is defined as

$$M(d)=\frac{1}{K}\sum_{l=0}^{1}\sum_{m=1}^{N/4-1} r\left(d+N/4+l\cdot N/2+m\right)\cdot r\left(d+N/4+l\cdot N/2-m\right) \tag{4}$$

where K is a normalization factor related to the length of CP, $r(d)$ is the received signal. Fig. 3 shows this timing metric as a function of timing offset for the case of no additive white Gaussian noise (AWGN) and no multipath distortion. We consider $N=1024$ and no CP. The graph is the result of an average over 50 randomly selected training symbols. These parameters are also used in Fig. 4. The graph shows two maximum values at $d=\pm N/4$ and a minimum at $d=0$.

To calculate the average, minimum and maximum values of the timing metric shown in Fig. 3, we assume that the average transmitted optical power is unity, i.e. $E\left\{x(n)\right\}=1$. Since $x(n)$ has a 'clipped Gaussian' distribution: it is zero with probability 0.5 and otherwise has a positive half Gaussian distribution. So $E\left\{x^2(n)\right\}=\pi$ [10]. For no noise and no multipath distortion, the received signal is equal to the transmitted signal and the timing metric in (4) becomes

$$M(d)=\frac{1}{K}\sum_{l=0}^{1}\sum_{m=1}^{N/4-1} x\left(d+N/4+l\cdot N/2+m\right)\cdot x\left(d+N/4+l\cdot N/2-m\right) \tag{5}$$

Equation (5) has the form of an inner summation of $N/4-1$ products of signal sample pairs and an outer summation over two values. The value of the metric depends on the total value of these summations which in turn depend on whether all, or a part of, the training symbol falls within the timing window. The maximum and minimum values of the timing metric as well as its average value are calculated in Appendix I. The normalized results are summarized below (given $CP=0$)

$$E\left[M(d)\right]=\begin{cases}1, & \text{when } d=\pm\dfrac{N}{4}\\ 0, & \text{when } d=0\\ \dfrac{1}{\pi+1}, & \text{when } d=\pm\dfrac{N}{2}\\ \dfrac{2}{\pi+1}, & \text{otherwise}\end{cases} \tag{6}$$

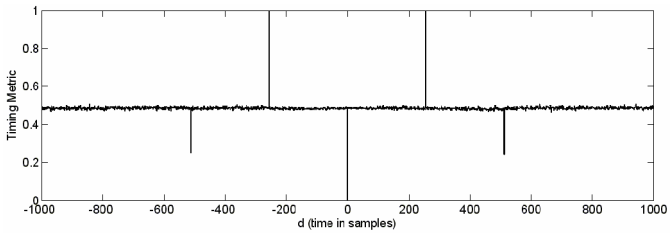

Fig. 3 Proposed timing metric with no AWGN and no multipath conditions (1024 subcarriers and zero CP length).

C. Impact of CP

One effect of the CP is to make two values of the timing metric at $d=\pm N/4$ unequal. Another effect is to cause an extra maximum at $d=-3N/4$. To explain these effects, consider the case where the CP length is $N/4$, the time domain training symbol vector $\mathbf{x}'_{train}$ is now given by

$$\mathbf{x}'_{train}=\left[0\quad (C^{mirror})_{clip}\quad 0\quad C_{clip}\quad 0\quad \left(-C^{mirror}\right)_{clip}\quad 0\quad (-C)_{clip}\quad 0\quad (C^{mirror})_{clip}\right] \tag{7}$$

Since $d=0$ is the start point of the useful training symbol given in (3), $d=-N/4$ is the start point of $\mathbf{x}'_{train}$. The maximum timing metric value at $d=-N/4$ includes $\left[0\quad (C^{mirror})_{clip}\quad 0\quad C_{clip}\right]$ and $\left[0\quad \left(-C^{mirror}\right)_{clip}\quad 0\quad (-C)_{clip}\right]$. Because the length of the correlated area is doubled, the maximum value is also increased. However, the correlated area does not change at $d=N/4$ and the timing metric value is therefore smaller than that at $d=-N/4$.

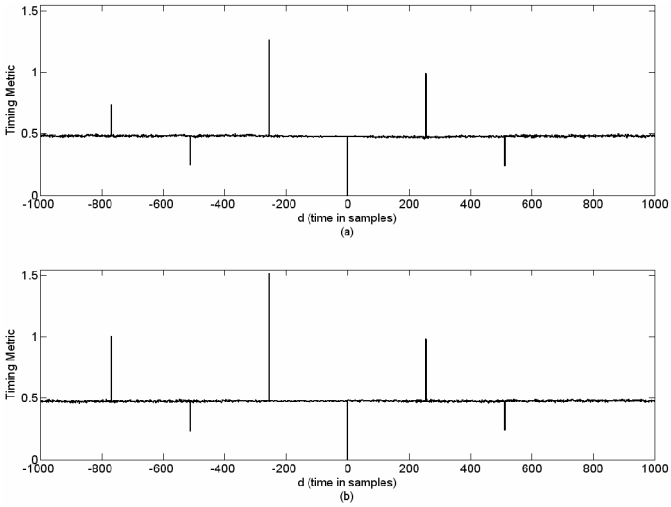

Fig. 4 Proposed timing metric (a) with *N*/8 CP lengh; and (b) with *N*/4 CP lengh (no AWGN and no multipath).

Fig. 4 (a) and (b) show the values of the timing metric, $M(d)$ with $\mathrm{CP} = N/8$ and $N/4$. The peak at $d = -N/4$ is larger than that at $d = N/4$. The longer the CP, the greater the difference between these two peaks becomes. Fig. 4 also shows another maximum at $d = -3N/4$. However, the length of the CP does not affect the positions of minimum values.

D. Two Detection Schemes

Using the timing metric shown in Fig. 4, the start of the training symbol can be located by either detecting the position of the minimum of the timing metric value located at $d = 0$ (Minimum Detection) or by detecting the position of the maximum value at $d = -N/4$ and then delaying it by $N/4$ samples (Maximum Detection). Both detection methods would suffer the interference from other sub-peaks. In [8], a combination of peaks has been used to find the timing offset.

IV. Simulation Results and Discussion

An OFDM system with 1024 subcarriers was simulated. Two channel models were used: line-of-sight (LOS) and a diffuse shadowed channel from [11]. It is assumed that there is one path in the LOS and three paths in the diffuse shadowed channel. The values of the taps h_i are given by

$$h_i = \frac{e^{-i}}{\sum_{i=0}^{L-1} e^{-i}} \tag{8}$$

In all cases, 50,000 monte carlo runs with the same training symbol were carried out to obtained the average of the mean and variance.

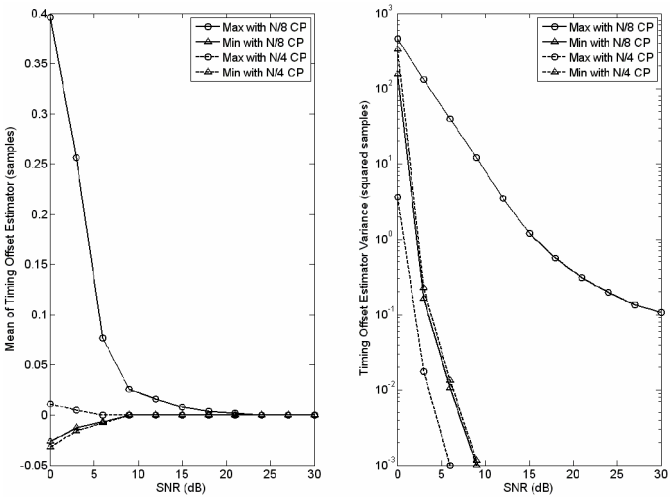

Fig. 5 Mean and variance of timing offset with different detection methods and different CP length in LOS channel.

Fig. 5 shows plots of the mean and variance of the timing offset for Maximum and Minimum Detection, with the length of the $\mathrm{CP} = N/8$ and $N/4$, for LOS channel against signal-to-noise ratio (SNR). As the SNR increases, the mean of the timing offset in each case approaches the optimum value, and the variance decreases. The Maximum Detection with $\mathrm{CP} = N/8$ has the worst performance. As the CP length increases to $N/4$, both the mean and variance improve significantly, attaining the best performance over all SNRs. For Minimum Detection, changing the length of the CP does not influence the results of mean and variance. When the CP is short, the Minimum Detection outperforms the Maximum Detection in terms of mean and variance of the timing offset. However, the performance of the Maximum Detection is better when a longer CP is used.

Fig. 6 shows the mean and variance of the Maximum and Minimum Detection in a diffuse shadowed channel. Again, Minimum Detection gives smaller mean and variance for when $\mathrm{CP} = N/8$. The variance of the Minimum Detection is smaller than that of the Maximum Detection for SNRs higher than 5dB. However when $\mathrm{CP} = N/4$, the performance of the Maximum detection improves significantly. The plots also show that, the change of the length of the CP has very small impact on the mean and the variance of the Minimum Detection.

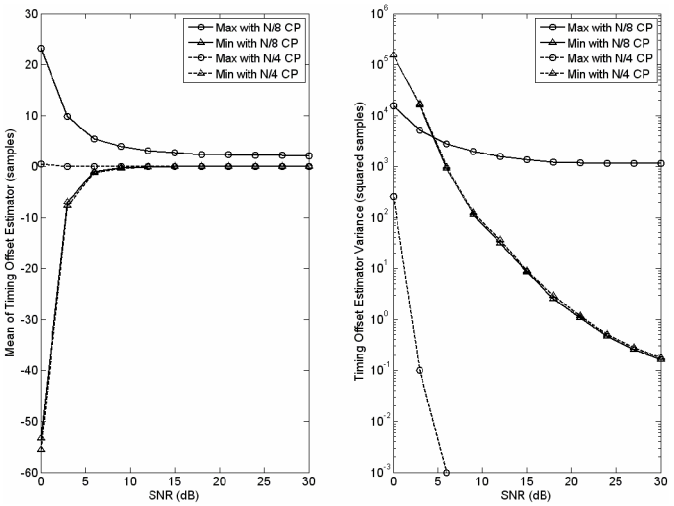

Fig. 6 Mean and variance of timing offset with different detection methods and different CP length in diffuse shadowed channel.

V. Conclusions

In this paper, we discuss the effect of CP length on the performance of a new synchronization method proposed for the ACO-OFDM systems. In particular, the effect of the CP on two detection criteria, Maximum and Minimum Detection, has been discussed. Simulation results were presented for these detection criteria in both a LOS and diffuse channel. It has been shown that timing offset estimation based on the Minimum Detection is less sensitive to the length of the CP employed than the one based on the Maximum Detection. While the timing offset detection scheme based on the

Maximum Detection with a longer CP gives a better performance, the system transmission efficiency will be decreased due to the longer length of the CP

ACKNOWLEDGMENT

This research is supported under the Australian Research Council's Discovery funding scheme (DP0772937).

REFERENCES

[1] J. Armstrong and A. J. Lowery, "Power efficient optical OFDM," *Electronics Lett.*, vol. 42, pp. 370-371, Mar. 2006.

[2] A. C. Boucouvalas, "Challenges in optical wireless communication," *Invited paper in Optics and Photonics News Magazine*, Aug. 2005.

[3] T. Ohtsuki, "Multiple-subcarrier modulation in optical wireless communications," *IEEE Commun. Mag.*, vol. 41, pp. 74-79, Mar. 2003.

[4] J. Armstrong, B. Schmidt, D. Kalra, H. A. Suraweera, and A. J. Lowery, "Performance of asymmetrically clipped optical OFDM in AWGN for an intensity modulated direct detection system," in *IEEE GLOBECOM '06*. San Francisco, CA, Nov./Dec. 2006. Accepted.

[5] T. Schmidl and D. Cox, "Robust frequency and timing synchronization for OFDM," *IEEE Trans. Commun.*, vol. 45, pp. 1613-1621, Dec. 1997.

[6] H. Minn, M. Zeng, and V. K. Bhargava, "On timing offset estimation for OFDM systems," *IEEE Commun. Lett.*, vol. 4, pp. 242-244, July 2000.

[7] B. Park, H. Cheon, C. Kang, and D. Hong, "A novel timing estimation method for OFDM systems," *IEEE Commun. Lett.*, vol. 7, pp. 239-241, May 2003.

[8] S. Tian, K. Panta, H. A. Suraweera, B. J. C. Schmidt, S. McLaughlin, and J. Armstrong, "A novel timing synchronization method for ACO-OFDM-based optical wireless communications," *submitted to IEEE Transactions on Wireless Communications*, June, 2007.

[9] J. M. Kahn and J. R. Barry, "Wireless infrared communications," *Proceedings of the IEEE*, vol. 85, pp. 265-298, Feb. 1997.

[10] X. Li, R. Mardling, and J. Armstrong, "Channel capacity of IM/DD optical communication systems and of ACO-OFDM," in *IEEE ICC '07*. Glasgow, UK, June 2007.

[11] J. M. Kahn, W. J. Krause, and J. B. Carruthers, "Experimental characterization of Non-Directed Indoor infrared channels," *IEEE Trans. Commun.*, vol. 43, pp. 1613-1623, April 1995.

[12] H. Ochiai and H. Imai, "On the distribution of the peak-to-average power ratio in OFDM signal," *IEEE Trans. Commun.*, vol. 49, pp. 282-289, Feb. 2001.

APPENDIX I

In this section, values of the timing metric given in (4) are calculated for different timing offset.

First the expected value when the training symbol is outside the timing window is calculated. In this case there is no correlation between the samples in the products in the inner summations and

$$\begin{aligned} E\{M(d)\} &= \frac{1}{K}\sum_{l=0}^{1}\sum_{m=1}^{N/4-1} E\{x(d+N/4+l\cdot N/2+m)\cdot x(d+N/4+l\cdot N/2-m)\} \\ &= \frac{1}{K}\sum_{l=0}^{1}\sum_{m=1}^{N/4-1} E\{x(d)\}\cdot E\{x(d)\} \\ &= \frac{2(N/4-1)}{K} \end{aligned} \tag{9}$$

The metric also has this value when the training symbol is within the timing window, but neither summation is centered about $N/4$, $N/2$ or $3N/4$. That is

$$E\{M(d)\} = \frac{2(N/4-1)}{K} \quad \text{for } d \neq 0, \pm N/4, \pm N/2 \tag{10}$$

For $d=0$, the timing metric is zero. This is can be proved by substituting $d=0$ in (5) and expanding the outer summation gives

$$M(0) = \frac{1}{K}\left(\sum_{m=1}^{N/4-1} x(N/4+m)\cdot x(N/4-m) + \sum_{m=1}^{N/4-1} x(N/4+N/2+m)\cdot x(N/4+N/2-m)\right) \tag{11}$$

To simplify this further it is necessary to use the properties of the training symbol $\mathbf{x}_{train}$. The first summation in (17) is over the first half of the training symbol which has the structure $\left[0 \;\; C_{clip} \;\; 0 \;\; \left(-C^{mirror}\right)_{clip}\right]$. Since $\left(-C^{mirror}\right)_{clip}$ is first negated and mirrored image of C before being clipped below zero, either $x(N/4+m)=0$ or $x(N/4-m)=0$. Thus each term in the first summation is zero. Using an identical argument this can also be shown to be true for the second summation in (11), so

$$M(0) = 0 \tag{12}$$

Using a similar approach the values of the timing metric at $d=\pm N/4$ can be calculated. Consider the case for $d=-N/4$. Then

$$\begin{aligned} M(-N/4) &= \frac{1}{K}\sum_{l=0}^{1}\sum_{m=1}^{N/4-1} x(+l\cdot N/2+m)\cdot x(+l\cdot N/2-m) \\ &= \frac{1}{K}\left(\sum_{m=1}^{N/4-1} x(+m)\cdot x(-m) + \sum_{m=1}^{N/4-1} x(+N/2+m)\cdot x(+N/2-m)\right) \end{aligned} \tag{13}$$

In this case the metric is the sum of two terms, one between the first quarter of the training symbol and the uncorrelated data which belongs to the last quarter of the preceding symbol and one over the center part of the training symbol which has structure $\left[0 \;\; \left(-C^{mirror}\right)_{clip} \;\; 0 \;\; (-C)_{clip}\right]$. Again, using the properties of mirroring and clipping, it can be shown that $x(+N/2+m) = x(+N/2-m)$ and that $x(m)=0$ with probability 0.5 and that $E\left\{x(m)^2 \,|\, x(m)\neq 0\right\} = 2\pi$. Thus

$$\begin{aligned} E\{M(-N/4)\} &= \frac{1}{K}\left(\sum_{m=1}^{N/4-1} E\{x(+m)\cdot x(-m)\} + \sum_{m=1}^{N/4-1} E\{x(+N/2+m)\cdot x(+N/2-m)\}\right) \\ &= \frac{1}{K}\left((N/4-1)+(N/4-1)\pi\right) \\ &= \frac{1}{K}(\pi+1)(N/4-1) \end{aligned} \tag{14}$$

This is consistent with Fig. 3 which shows a maxima at $d=\pm N/4$. Let $K=(\pi+1)(N/4-1)$, the average level is $2/(\pi+1)$. It can be derived similarly that the values at $d=\pm N/2$ are $1/(\pi+1)$.